PHILOSOPHICAL TRANSACTIONS OF THE ROYAL SOCIETY A

Phil. Trans. R. Soc. A (2008) **366**, 3445–3462
doi:10.1098/rsta.2008.0133
Published online 16 July 2008

Monitoring of chloride and activity of glycine receptor channels using genetically encoded fluorescent sensors

By Marat Mukhtarov[1,†], Olga Markova[1,†], Eleonore Real[2,‡], Yves Jacob[2], Svetlana Buldakova[1] and Piotr Bregestovski[1,*]

[1]*Institut de Neurobiologie de la Méditerranée (INMED), INSERM U901, Parc Scientifique de Luminy, 13273 Marseille Cedex 09, France*
[2]*Unit of Genetics, Papillomavirus and Human Cancer, Department of Virology, Pasteur Institute, 25 rue du docteur Roux, 75724 Paris, France*

Genetically encoded probes have become powerful tools for non-invasive monitoring of ions, distributions of proteins and the migration and formation of cellular components. We describe the functional expression of two molecular probes for non-invasive fluorescent monitoring of intracellular Cl ($[Cl]_i$) and the functioning of glycine receptor (GlyR) channels. The first probe is a recently developed cyan fluorescent protein–yellow fluorescent protein-based construct, termed Cl-Sensor, with relatively high sensitivity to Cl ($K_{app} \sim 30$ mM). In this study, we describe its expression in retina cells using *in vivo* electroporation and analyse changes in $[Cl]_i$ at depolarization and during the first three weeks of post-natal development. An application of 40 mM K^+ causes an elevation in $[Cl]_i$ of approximately 40 mM. In photoreceptors from retina slices of a 6-day-old rat (P6 rat), the mean $[Cl]_i$ is approximately 50 mM, and for P16 and P21 rats it is approximately 30–35 mM. The second construct, termed BioSensor-GlyR, is a GlyR channel with Cl-Sensor incorporated into the cytoplasmic domain. This is the first molecular probe for spectroscopic monitoring of the functioning of receptor-operated channels. These types of probes offer a means of screening pharmacological agents and monitoring Cl under different physiological and pathological conditions and permit spectroscopic monitoring of the activity of GlyRs expressed in heterologous systems and neurons.

Keywords: fluorescent probes; real-time optical detection; patch clamp; glycine receptor; retina; electroporation

1. Introduction

Development of imaging techniques and specific probes has opened new avenues for non-invasive monitoring of ion and protein distributions and of the formation and migration of cellular components. Genetically encoded probes represent

* Author for correspondence (pbreges@inmed.univ-mrs.fr).
† These authors contributed equally to this work.
‡ Present address: Laboratory of Neurogenetics and Behavior, Rockefeller University, 1230 York Avenue, Box 63, NY 10021, USA.

One contribution of 12 to a Theme Issue 'Biomedical applications of systems biology and biological physics'.

particularly powerful tools for these tasks. These probes are non-toxic, capable of staying in cells for a long time and can be expressed in specific cellular compartments. These fluorescent optical probes have been successfully used for the visualization of ions and proteins in various cell types (Siegel & Isacoff 1997; Gandhi *et al.* 2000; Demaurex & Frieden 2003; Miyawaki 2003; Gorostiza *et al.* 2007).

During the last decade, several genetically encoded probes for monitoring of intracellular Cl have been developed. Such probes are based on the fact that yellow fluorescent protein (YFP) is quenched by small anions and they may be used as very weak Cl sensors (Wachter & Remington 1999). YFP mutants with enhanced Cl sensitivity and accelerated responses have been proposed for monitoring the changes in halide fluxes in cells (Jayaraman *et al.* 2000; Galietta *et al.* 2001*a*). These mutants also exhibit good pH sensitivity with apparent pK_a values from 7.0 to 8.0, depending on the Cl concentration (Jayaraman *et al.* 2000).

YFP-based probes have been successfully used for quantitative screening of chloride transport in different cells (Galietta *et al.* 2001*b*; Rhoden *et al.* 2007) and for high-throughput screening of Cl-selective glycine and $GABA_A$ receptor channels (Kruger *et al.* 2005). Also transgenic mice expressing YFP were generated and used for the analysis of glutamate-induced changes in intracellular Cl and pH (Metzger *et al.* 2002; Slemmer *et al.* 2004).

However, these probes do not allow estimation of the intracellular Cl concentration ($[Cl]_i$). This problem was solved by Kuner & Augustine (2000) who constructed a fusion protein containing YFP combined with the Cl-insensitive cyan fluorescent protein (CFP). This construct, termed Clomeleon, allows ratiometric estimation of $[Cl]_i$ in neurons using fluorescence emission ratio (Kuner & Augustine 2000). The sensitivity of this protein to Cl is relatively low ($K_{app} > 160$ mM), which is far from the physiological range of $[Cl]_i$ in nervous systems of vertebrates (approx. 5–40 mM; Krapf *et al.* 1988; Rohrbough & Spitzer 1996; Tyzio *et al.* 2006; Markova *et al.* 2008).

Recently we have developed a new CFP–YFP-based construct, termed Cl-Sensor, with a relatively high sensitivity to Cl ($K_{app} \sim 30$ mM) due to triple YFP mutant (Markova *et al.* 2008). The construct allows ratiometric monitoring using fluorescence excitation ratio. It also exhibits good pH sensitivity with pK_a ranging from 7.1 to 8.0 pH units at different Cl concentrations. This genetically encoded indicator was used for the non-invasive estimation of $[Cl]_i$ in cultured Chinese hamster ovary cells (CHO cells) and in neurons of primary hippocampal cultures (Markova *et al.* 2008). In the present study, we describe additional observations on the functional expression of the Cl-Sensor.

Particularly important is the development of genetically encoded probes for monitoring the activity of ionic channels. The analysis of ion-channel function and its modulation by pharmacological compounds is based mainly on electrophysiological observations. Although highly informative in single-cell recordings, these techniques, in general, have low throughput, limiting the number of agents that can be conveniently studied. Genetic incorporation of molecules that change their fluorescence on activation of receptor-operated channels could overcome this problem. However, the development of such molecular tools is a highly challenging task. Here we present a new construct, termed BioSensor-GlyR, that allows monitoring of the activation of Cl-selective glycine receptor (GlyR) channel.

The GlyR is a hetero-pentameric ion channel protein that mediates hyperpolarization of the mature postsynaptic nerve cell due to an increase in the Cl conductance and the subsequent entry of Cl ions (Hamill *et al.* 1983). GlyR belongs to the superfamily of ligand-gated ion channel proteins that also include ionotrophic GABA, acetylcholine and serotonin receptors (Ortells & Lunt 1995). GlyRs have several important functions including movement control, pain sensation and sensory information processing. Several heritable diseases, including hyperekplexia, originate from GlyR dysfunction (Becker 1990).

We constructed the new molecular probe by introducing into the cytoplasmic domain of GlyR a CFP–YFP-based Cl-Sensor. This insertion did not change the functional properties of GlyR. The application of glycine to cells expressing this chimera channel induced fluorescence changes, whose intensity correlated with the amplitude of glycine-induced currents. This construct, termed BioSensor-GlyR, is the first molecular probe for non-invasive monitoring of receptor-operated channel functioning. It offers a means of screening pharmacological agents and monitoring Cl or GlyR activity under different physiological and pathological conditions.

2. Methods

(*a*) *Cell cultures and transfection*

Experiments were carried out on three cell lines, human embryonic kidney cells (HEK-293), CHO-K1 and baby hamster kidney cells (BHK-21), and on slices from the retina of rats. CHO-K1 cells were obtained from the American Type Tissue Culture Collection (ATCC, Molsheim, France).

Cells were prepared and maintained as previously described (Fucile *et al.* 2000; Chudotvorova *et al.* 2005). Transfections were performed using the Lipofectamine transfection protocol (Gibco, Invitrogen) with some modifications. Briefly, cells were incubated in a solution containing 300 µl of Opti-MEM, 1 µl of Magnetofection CombiMag (OZ Bioscience, France), 6 µl of Lipofectamine reagent 2000 (Invitrogen) and 1 µg of the Cl-Sensor or BioSensor-GlyR constructs. After 30 min of incubation at 37°C on a magnetic plate (OZ Bioscience), the transfection mixture was replaced with fresh growth medium supplemented with 1 µm of strychnine (to prevent Cl influx through expressed GlyRs). Cells were used in the experiments 24–76 hours after transfection.

(*b*) In vivo *electroporation and slices preparation*

Experiments were conducted on Wistar rats. For *in vivo* electroporation, we used the protocol described previously (Matsuda & Cepko 2004) with a few modifications. In brief, newborn Wistar rat pups were anaesthetized by chilling on ice. A small incision was made in the eyelid and sclera near the lens with a 30 gauge needle. A Hamilton syringe with a 32 gauge blunt-ended needle was filled with phosphate-buffered saline (PBS) solution containing Cl-Sensor complementary deoxyribonucleic acid (cDNA; 3 µg μl^{-1}) and 0.1 per cent fast green as a tracer. Under a dissecting microscope, 1 µl of cDNA was injected through the incision usually into right eye. Then tweezer-type electrodes (model 520, 7 mm diameter, BTX, San Diego, CA, USA) briefly soaked in PBS were

placed to softly hold the heads of the pups. Using a pulse generator, ECM830 (BTX), square pulses in amplitude 120 mV and 50 ms duration were applied seven times with interval 1 s. After 5 min break, this electroporation protocol was repeated.

Recording of fluorescent signals was carried out on retina slices from electroporated animals of post-natal age 6–21 days (P6–P21). Animals were anaesthetized with ether and killed by decapitation in agreement with the European Directive 86/609/EEC requirements. Subsequently, an eye was enucleated and hemisected. After the vitreous body was removed, the pieces of retina were cut into 200 μm thick slices by a McILWAIN tissue chopper (The Mickle Laboratory Engineering Co. Ltd, England).

For monitoring Cl-Sensor fluorescence, slices were placed in the chamber under the upright microscope (Axioskop, Zeiss, Germany) and were superfused (1.0–1.5 ml min^{-1}) with oxygenated solution containing (in mM): NaCl, 125; KCl, 3.5; $CaCl_2$, 2; $MgCl_2$, 1.3; NaH_2PO_4, 1.25; $NaHCO_3$, 26; and glucose, 10; equilibrated at pH 7.3 with 95 per cent O_2 and 5 per cent CO_2. The solution with elevated external K^+ concentration contained 40 mM KCl and 88.5 mM NaCl. For 'low-Cl' external solutions, NaCl and KCl salts were substituted with the corresponding gluconate salts.

Prior to recording, slices were incubated at room temperature (22–25°C) for at least 1 hour to allow recovery.

(*c*) *Electrophysiological recordings*

Whole-cell recordings were conducted on HEK-293 and CHO-K1 cells using an EPC-9 amplifier (HEKA Elektronik, Germany) at room temperature (22–25°C). Cells were continuously superfused with external solution through an independent tube. The external solution contained (mM): NaCl, 140; $CaCl_2$, 2; KCl, 2.8; $MgCl_2$, 2; HEPES, 20; glucose, 10; pH 7.3; 315 mOsm. The patch pipette solution contained (mM): KCl (0–150) or KGluconate (0–150); $MgCl_2$, 2; MgATP, 2; HEPES/KOH, 20; BAPTA, 1; pH 7.3; 290 mOsm. To vary the Cl concentration from 0 to 150 mM, a combination of KGluconate and KCl at a constant K^+ concentration was used. Pipettes were pulled from borosilicate glass capillaries (Harvard Apparatus Ltd, USA) and had resistances of 5–7 MΩ.

Glycine was applied locally from pipettes using pressure pulses with 'Picospritzer' (General Valve Corporation, USA). The pipettes were filled with an external solution containing 1 mM glycine and were placed 50–100 μm from the soma of the cells.

(*d*) *Real-time fluorescence imaging*

Fluorescence images were acquired using a customized digital imaging microscope. Excitation of cells at various wavelengths was achieved using a 1 nm bandwidth polychromatic light selector equipped with a 100 W xenon lamp (PolychromeII; Till Photonics, Germany). Light intensity was attenuated using neutral density filters. A dichroic mirror (495 nm; Omega Optics, USA) was used to deflect light onto the samples. Fluorescence was visualized using an upright microscope (Axioskop) equipped with an infinity-corrected 60× water-immersion objective (n.a. = 0.9; LumPlanFL, Olympus, USA). Fluorescent-emitted light passed to a 12 bit charge-coupled device digital camera system equipped with an

image intensifier (PentaMax512EEV-GENIV, Princeton Instruments, USA). Images were acquired on a computer via a DMA serial transfer. All peripheral hardware control, image acquisition and image processing were achieved using customized routines provided by MetaFluor software (International Imaging, USA). The average fluorescence intensity of each region of interest was measured. Mean background fluorescence (measured from a non-fluorescent area) was subtracted and the ratio intensities (F_{480}/F_{440}) were determined. Depending on the experimental task, the frequency of acquisition varied from 20 to 0.1 Hz and duration of excitation was 10–100 ms.

(*e*) *Insertional mutagenesis for production of functional GlyR channels fused with YFP in the cytoplasmic domain*

In order to determine a functionally neutral position for insertion in the long cytoplasmic loop of the human α1 GlyR subunit, we used the linker-scanning system from New England Biolabs (GPS-LS). Mutagenesis was realized by a Tn7-based transposition reaction introducing, at random positions throughout the 270 bp target DNA, a 15 bp linker containing a *Pme I* restriction site. This procedure generates an insertion of five amino acids in four out of six frames; the remaining two frames had the thymine–adenine–adenine (TAA) stop codon. Saturation mutagenesis was realized using this approach; less than 5×10^4 colonies were collected, constituting a mini-library of GlyR-loop mutants cloned into the bacterial T7 promoter-based expression vector pIVEX 2.3 (Roche). The enhanced YFP (eYFP; Clontech) coding sequence amplified by polymerase chain reaction (PCR) using a set of degenerate primers with *Pme I* sites was inserted into the long cytoplasmic domain of GlyR at the linker positions. *Escherichia coli* clones with in-frame insertion were selected based on their fluorescence. After sequencing of 96 individual randomly picked clones, eight insertions were chosen distributed along the region encompassing residues E331-K378, which is the most divergent between human and zebrafish α1 and α2 GlyR subunits and thus less likely to be structurally constrained. The corresponding GlyR-loop fragments containing an eYFP insertion were introduced using *BspH I* cloning in the full-length GlyR gene cloned in a mammalian expression vector (derived from pCineo; Promega). Each construct was confirmed by sequencing, amplified in *E. coli* DH5α and purified by chromatography (Qiagen) to be transfected in HEK 293 cells for electrophysiological validation. Among these constructs, the insertion of the eYFP between residues P367 and A368 displayed the highest level of fluorescence and was electrophysiologically neutral, i.e. it did not change the functional properties of GlyR. This neutral position for insertion was used to produce the BioSensor-GlyR construct. The chimeric GlyR was realized by inserting, in frame at the 5′ and 3′ ends of the Cl-Sensor, two PCR-generated DNA fragments encoding, respectively, for GlyR amino acids 1–367 (*Xba I* fragment cloned in the *Nhe I* unique site of the Cl-Sensor vector) and GlyR amino acids 368–421 (*Bgl II* fragment cloned in the *BamH I* unique site of the Cl-Sensor vector); the expression of the resulting BioSensor-GlyR transgene was under the control of the CMVie promoter from the initial backbone of the Cl-Sensor vector.

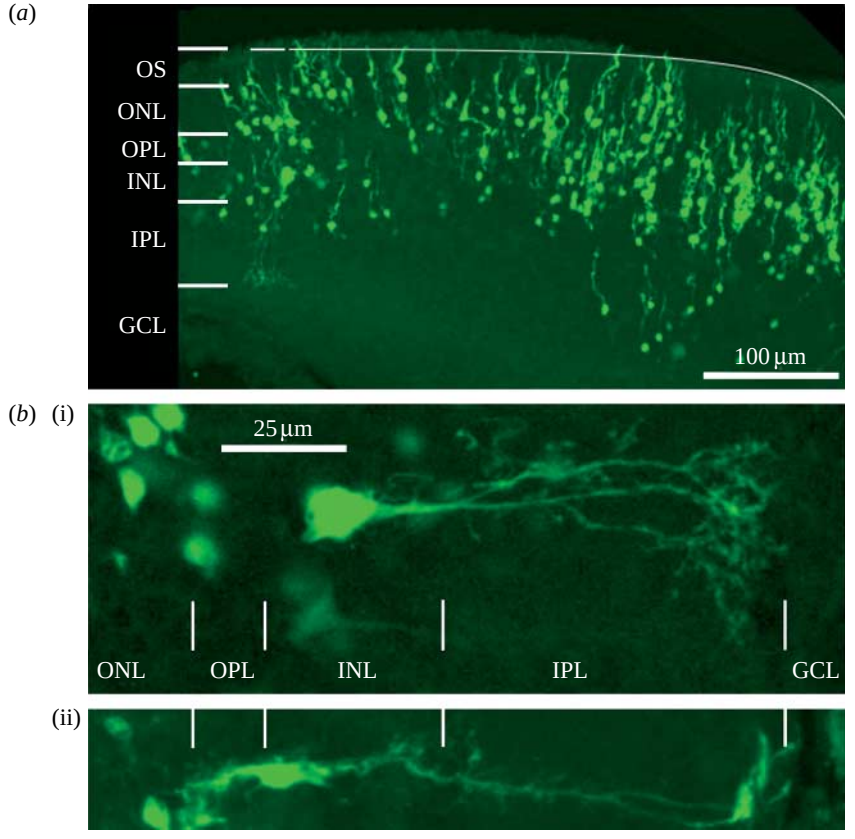

Figure 1. Expression of fluorescent protein in rat retina slices. (*a*) Example of confocal imaging photomicrograph showing a vertical section of a rat retina that was electroporated with green fluorescent protein. (*b*) Examples of (i) amacrine and (ii) bipolar cell at higher magnification. Retinal layers are indicated: OS, outer segment; ONL, outer nuclear layer; OPL, outer plexiform layer; INL, inner nuclear layer; IPL, inner plexiform layer; GCL, ganglion cell layer.

3. Results

(*a*) *Non-invasive monitoring of intracellular Cl in retinal cells using Cl-Sensor*

To develop the technique for non-invasive monitoring of $[Cl]_i$ in retina slices, we expressed Cl-Sensor using the cDNA delivering method originally proposed by Matsuda & Cepko (2004). For this, Cl-Sensor cDNA was introduced in the retina of neonatal rats using electroporation protocol (see §2). For fluorescent analysis, slices of retina (200 µm) were prepared from electroporated animals at the age P6–P21. As the control, we also electroporated retinas with green fluorescent protein (GFP; figure 1*a*). No difference in the pattern of distribution of Cl-Sensor and GFP was observed. The expression of fluorescent proteins was observed in a wide area with particularly massive fluorescence in the photoreceptor layer. Some cells from the inner nuclear layer (amacrine and bipolar cells) also exhibited robust expression of fluorescent proteins (figure 1*b*). For non-invasive estimation of $[Cl]_i$, we primarily used photoreceptors expressing Cl-Sensor.

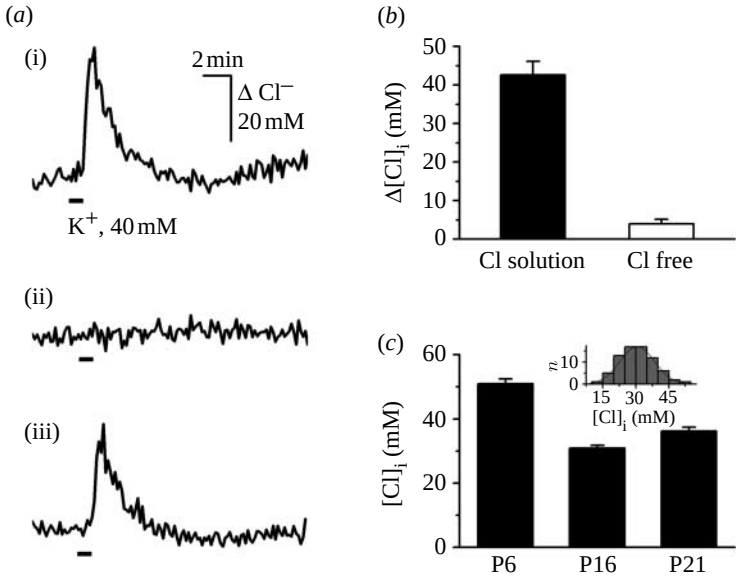

Figure 2. Non-invasive monitoring of $[Cl]_i$ changes in retinal cells. (*a*) Example of $[Cl]_i$ changes in response to 40 mM K^+-induced depolarization in solutions containing (i, iii) 135 mM Cl and (ii) 6.5 mM Cl (Cl free). Photoreceptor cell from a P16 rat retina slice. 'High-K^+' solution was bath applied. (*b*) Average changes in $[Cl]_i$ following 'high-K^+'-induced depolarization in normal (black bar) and low-Cl (white bar) solutions. Data are means $\pm$ s.e.m. of seven photoreceptor cells. The base level of $[Cl]_i$ before depolarization was 36 ± 5 mM ($n=7$). (*c*) Age-dependent changes of $[Cl]_i$ in retinal cells. Average data from P6 ($n=64$), P16 ($n=73$) and P21 ($n=63$) rat retina slices are shown. Inset presents the histogram of distribution of $[Cl]_i$ in photoreceptor cells from P16 rat retina slices.

(i) *Depolarization-induced Cl changes in photoreceptor cells*

Our preliminary observations demonstrated that depolarization induced by bath application of 40 mM K^+ causes strong elevation of $[Cl]_i$ in photoreceptor cells (Markova *et al.* 2008). In this section we present additional observations of this effect.

An external solution containing 40 mM K^+ was bath applied to retina slices from P14 to P16 rats and fluorescence ratios (F_{480}/F_{440}) were monitored at a low acquisition rate (0.1 Hz). As illustrated in figure 2*a*, in the external solution containing normal Cl concentration (approx. 135 mM), K^+-induced depolarization caused changes in the fluorescence ratio corresponding to an increase in $[Cl]_i$ of approximately 40 mM. By contrast, in the low-Cl solution, containing approximately 5 mM Cl, this increase was strongly and reversibly suppressed. On average, in normal Cl-containing solution, application of 40 mM K^+ caused an elevation in $[Cl]_i$ of 43 ± 3 mM ($n=7$; figure 2*b*). In the low-Cl solution, this increase was only 4 ± 1 mM (figure 2*b*). The mean background level of Cl in photoreceptors before depolarization was 36 ± 5 mM ($n=7$), indicating that application of high K^+ caused an elevation of $[Cl]_i$ to more than 70 mM.

These results show that depolarization can strongly modify $[Cl]_i$, supporting previous observations that $[Cl]_i$ is a highly dynamic parameter depending on the activation of different ionic channels and transporters (Rohrbough & Spitzer 1996; Slemmer *et al.* 2004; Tyzio *et al.* 2007).

(ii) *Age-dependent changes of* $[Cl]_i$ *in photoreceptors of rat retina slices*

Using non-invasive monitoring of $[Cl]_i$, we have recently demonstrated that the photoreceptors from retinas of P14–P15 rats contain relatively high $[Cl]_i$ of more than 30 mM (Markova *et al.* 2008). It is well documented that the $[Cl]_i$ in brain slices of hippocampus and other rat brain areas change significantly during the first two weeks of post-natal development (Ben-Ari *et al.* 2007). Hence, we analysed the age-dependent changes of $[Cl]_i$ in photoreceptor cells. Fluorescent spectra were recorded and $[Cl]_i$ was calculated, as described earlier (Markova *et al.* 2008).

As shown in figure 2*c*, in photoreceptors from P6 rat retina slices, the mean $[Cl]_i$ value was 51 ± 2 mM ($n=64$). At P16, this value decreased to 31 ± 1 mM ($n=73$; figure 2*c*). Thereafter, the $[Cl]_i$ did not change significantly, and at P21 it was 36 ± 1 mM ($n=63$; figure 2*c*). As shown in the inset of figure 2*c*, the distribution of $[Cl]_i$ in photoreceptor cells represents a good fit to a Gaussian curve.

These observations confirm previous results indicating that photoreceptor cells possess relatively high $[Cl]_i$ (Thoreson *et al.* 2002; Thoreson & Bryson 2004; Markova *et al.* 2008). Our data also show that the Cl-Sensor represents an effective tool for $[Cl]_i$ monitoring in different conditions and thus provides a useful starting point for development tools that allow non-invasive monitoring of the activity of Cl-selective receptor-operated channels.

(*b*) *Development of BioSensor for spectroscopic monitoring of GlyR channel activity*

To obtain a new genetically encoded tool that allows spectroscopic monitoring of channel activity in live cells, we used the fact that GlyR is a Cl-selective protein. Our strategy involved the following three steps:

(i) determination of a region of the cytoplasmic domain of GlyR, which allows the introduction of a foreign protein of several hundred amino acids without changing the functional properties of the receptor,
(ii) introduction of the Cl-Sensor in this region, and
(iii) analyses of the functional and spectroscopic properties of this construct.

(i) *Production of functional GlyR channels fused with YFP in the cytoplasmic domain*

Previously, we constructed a functional GlyR fused with GFP and used it to study the GlyR distribution in living cells (David-Watine *et al.* 1999). In this earlier construct, GFP was fused to the extracellular domain of GlyR. For monitoring changes in the intracellular Cl caused by the activation of anion-selective channels, it was necessary to position Cl-Sensor in the vicinity of these channels on the cytoplasmic side of the membrane.

To achieve this, we first developed a strategy for the incorporation of YFP into the long cytoplasmic domain of GlyR. Using insertional mutagenesis, we generated a library of random mutants of the GlyR cytoplasmic loop to enable the incorporation of YFP into the long cytoplasmic domain of the human α1 subunits of GlyR (see §2).

From the resulting mutants, several candidates were selected for electrophysiological analysis. cDNAs of each GlyR-YFP construct were transfected into HEK-293 cells. Whole-cell recording techniques revealed just one functional clone with properties similar to those of the wild-type GlyR (figure 3).

Confocal imaging revealed strong membrane and partial intracellular (Golgi apparatus and endoplasmic reticulum) fluorescence distribution of this GlyR-YFP construct (figure 3*a*(i)). This is in contrast to GFP, which exhibits homogeneous distribution in cells (figure 3*a*(ii)). Analysis of concentration dependences showed that the EC_{50} and maximal currents evoked by saturated concentrations of glycine are similar for cells expressing GlyR-YFP and wild-type GlyR (figure 3*b*,*c*).

These results demonstrate that the fusion of YFP to the cytoplasmic domain of GlyR gives a channel whose distribution is primarily transmembrane and with functional properties similar to those of the wild-type. This construct was used for obtaining the functional GlyR capable of changing fluorescence upon activation.

(ii) *Construction of BioSensor-GlyR*

The design of the chimeric Biosensor-GlyR transgene was based on the observation of a functionally neutral position in the GlyR cytoplasmic loop, which accommodates YFP insertion. Thus, in order to produce a functional GlyR capable of changing fluorescence upon activation, the previously developed Cl-Sensor was inserted instead of YFP into the long cytoplasmic domain of GlyR (figure 4*a*). The resulting construct that we call BioSensor-GlyR was transiently expressed in CHO, BHK and HEK cells using lipofectamine transfection.

In whole-cell recordings of cells expressing BioSensor-GlyR, rapid application of glycine elicited ionic currents with kinetics similar to those of wild-type GlyR (figure 4*c*). Concentration dependences for BioSensor-GlyR and wild-type GlyR were also similar (figure 4*d*). Over all recorded cells, the values of EC_{50} obtained from concentration dependences largely overlapped: 30–210 μM for wild-type ($n=44$) and 70–300 μM for cells expressing BioSensor-GlyR ($n=8$). Analyses of the *I*–*V* relations revealed that for cells expressing BioSensor-GlyR, the reversal potential for glycine-induced currents closely followed reversal potential for chloride (E_{Cl}) (figure 4*b*).

The main functional properties of BioSensor-GlyR, i.e. kinetics, agonist sensitivity and Cl selectivity, are thus similar to those of the wild-type GlyR.

(iii) *Functional properties of BioSensor-GlyR*

The fluorescence spectral properties of BioSensor-GlyR were examined by simultaneous monitoring of fluorescence signals and whole-cell recordings with different Cl concentrations in the pipette solution (0–150 mM). To vary the Cl concentration from 0 to 150 mM, a combination of KGluconate and KCl at a constant K^+ concentration was used.

The excitation spectra (410–490 nm) were recorded and for the convenience of analysis each spectrum was normalized (Markova *et al.* 2008). At high internal Cl (140 mM), normalized spectra showed a maximal peak at approximately 450 nm with a close to minimum at approximately 490 nm. Lowering the Cl concentration in the pipette solutions resulted in an elevation of normalized

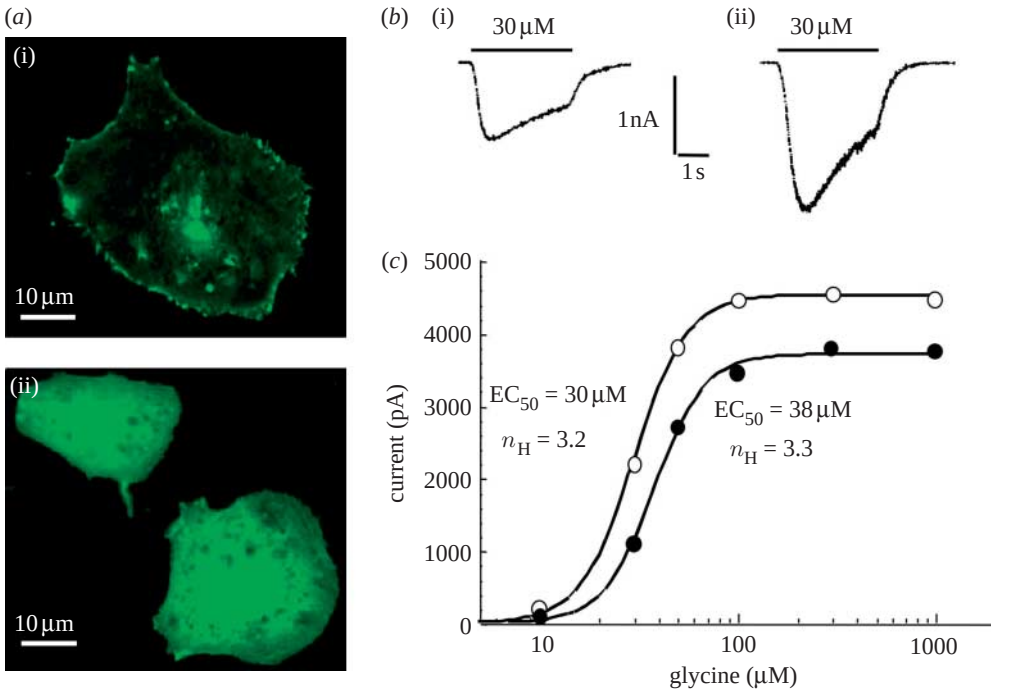

Figure 3. Functional GlyR-YFP construct with YFP at the long cytoplasmic domain. (*a*) Fluorescence distribution in HEK-293 cells expressing either (i) GlyR-YFP or (ii) wild-type GFP. Fluorescence images were obtained via a confocal microscope with a *z*-plane depth of 0.4 µm. Note the distribution of GlyR-YFP fluorescence predominantly in the membrane. (*b*) Traces of ionic currents measured from HEK-293 cells transfected with (i) the human α1 GlyR subunit or (ii) the GlyR-YFP construct. Glycine (30 µM) was applied during the time indicated by bars above traces. $V_h = -50$ mV. (*c*) Dose–response relationships for two cells expressing either the wild-type GlyR (filled circles) or GlyR-YFP construct (open circles). Note similar maximal current and EC_{50} values for the two receptors.

fluorescence intensity at 480 nm and reduction at 450 nm (figure 5*a*). Normalized spectra had a common point near 465 nm (figure 5*a*). For every spectrum the intensity at this point was Cl independent. Thus, BioSensor-GlyR can be used as a ratiometric excitation wavelength indicator.

Simultaneous monitoring revealed that the amplitude and direction of fluorescence signals correlated with the amplitude and direction of glycine-induced currents (figure 5*b–d*). The relationships between the amplitude of glycine-induced currents and the changes in fluorescence were nearly linear (figure 5*b*).

To simulate synaptic conditions, we applied short pressure pulses of glycine to the surface of recorded cells. Figure 5*c* shows an ionic current of approximately 300 pA, induced by a pulse of glycine, causing a detectable fluorescence signal. This current is of similar magnitude to glycinergic synaptic currents recorded in motor neurons of the hypoglossal nucleus (Mukhtarov *et al.* 2005), in neurons of rat ventrobasal thalamus (Ghavanini *et al.* 2006) and in embryonic muscle cells (Borodinsky & Spitzer 2007).

These results demonstrate that BioSensor-GlyR is a good probe for spectroscopic monitoring of GlyR activation in live cells.

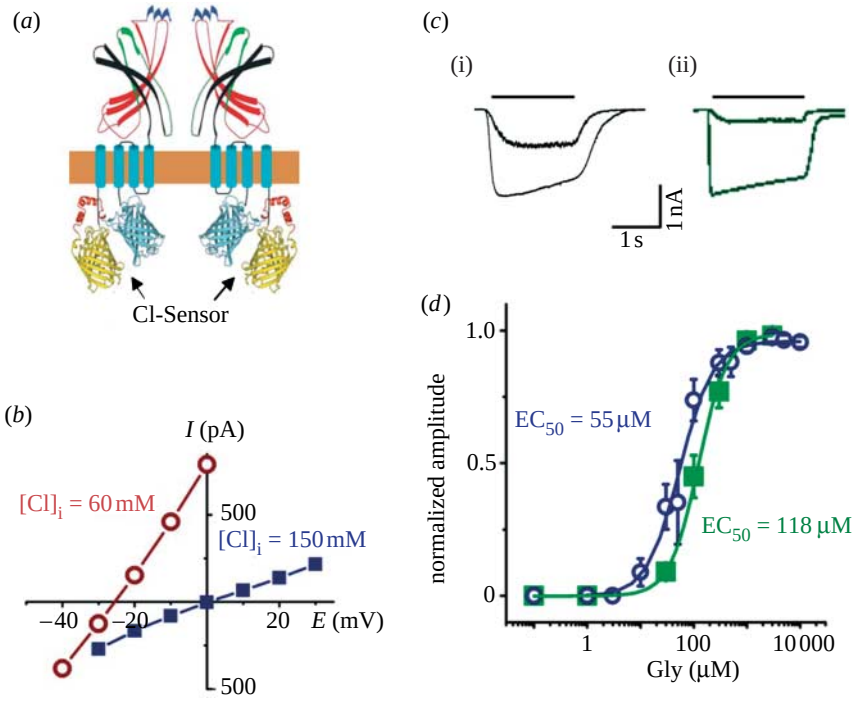

Figure 4. Production of functional BioSensor-GlyR construct. (*a*) Scheme of BioSensor-GlyR construct. Two subunits are shown. (*b*) *I–V* relations for glycine-induced currents in two CHO cells expressing BioSensor-GlyR. Recording pipettes contained solutions that gave theoretical reversal potential for chloride (E_{Cl}) values of 0 mV (squares) and −25 mV (circles). The external Cl concentration was 150 mM; pipette Cl is indicated on the graph. Note that reversal potentials correspond closely to the theoretical E_{Cl} values predicted by the Nernst equation. (*c*) Superimposed traces of whole-cell currents induced by rapid application of glycine (30 or 300 µM). CHO cells transfected with either (i) wild-type human GlyR or (ii) BioSensor-GlyR. Holding potential (V_h) = −30 mV. External and pipette solutions contained 150 mM Cl. (*d*) Dose–response curves obtained from cells expressing either wild-type human GlyR (circles) or BioSensor-GlyR (squares). Each point represents the mean ± s.e.m. of 8–10 cells.

4. Discussion

In biological organisms, the concentration of Cl and its membrane permeability are highly regulated by a variety of Cl-selective channels and Cl transporters. Dysfunction of these proteins results in various diseases. For instance, the most prevalent lethal genetic disease, cystic fibrosis (Kere *et al.* 1999), arises from mutation in the specific regulator of Cl permeability: cystic fibrosis transmembrane conductance regulator protein (CFTR). This voltage-independent Cl channel is found in the epithelial cells of many tissues (intestine, lung, reproductive tract, pancreatic ducts). Mutation in the gene encoding CFTR affects one in 2000–2500 people (Ashcroft 2000). Several other human diseases have been linked to dysfunctional Cl homeostasis: myotonia congenita (Koch *et al.* 1992); congenital chloride diarrhoea (Kere *et al.* 1999); inherited hypercalciuric nephrolithiasis (Lloyd *et al.* 1996); Bartter's and Gitelman's syndromes

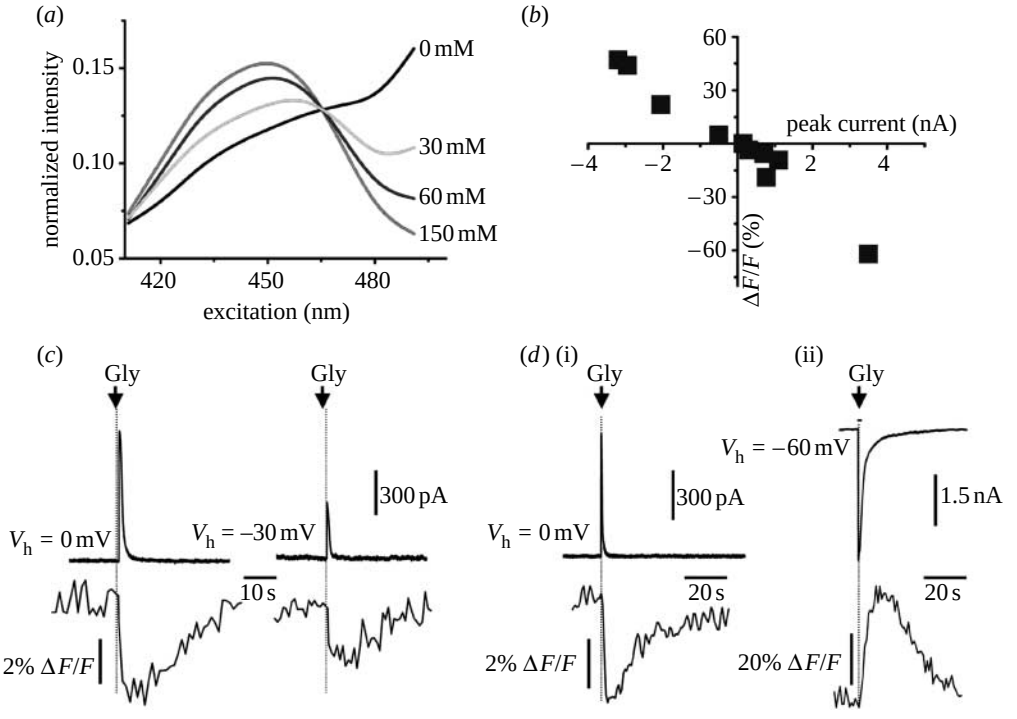

Figure 5. Fluorescence spectra and glycine-induced responses of BioSensor-GlyR. (*a*) Normalized spectra of BioSensor-GlyR. Whole-cell recording from BHK cells with pipettes containing different Cl concentrations (shown in the graph). Note that spectra intersect at a common point (465 nm). (*b*) Relationships between the amplitude of glycine-induced currents and changes in fluorescence of BioSensor-GlyR at 480 nm. The amplitude of currents was regulated by the changing of V_h. (*c*,*d*) Examples of simultaneous fluorescence and whole-cell recordings from cells expressing BioSensor-GlyR. Transient responses were initiated by pressure application of 1 mM glycine. Upper panels: whole-cell recordings of currents. Bottom panels: corresponding fluorescence changes at 480 nm. (*c*) Recordings at two holding potentials (0 and −30 mV) with a pipette nominally containing 0 mM Cl. Duration of glycine application was 100 ms. Note that the increase in amplitude of fluorescence transients corresponds to the elevation in glycine-induced current amplitude. (*d*) (i) Recordings with a pipette containing nominally 0 mM Cl. Duration of glycine application was 10 ms. (ii) Recordings with a pipette containing 150 mM Cl.

(Simon & Lifton 1996); hyperekplexia, also known as startle disease (Shiang *et al.* 1993); and epilepsy (Treiman 2001). Technical difficulties in the measurement of Cl flux in live cells hamper elucidation of the mechanisms regulating Cl in both physiological and pathological conditions.

Non-invasive monitoring of $[Cl]_i$ is a challenging task owing to two main difficulties. The first is the relatively small difference in transmembrane Cl concentrations. In mammalian organisms, extracellular Cl concentration is approximately 150 mM. Intracellular concentration of this anion strongly varies depending on the cell type, stage of ontogenetic development and pathological condition. It is usually in the range of 5–40 mM (Krapf *et al.* 1988; Rohrbough & Spitzer 1996; Tyzio *et al.* 2006; Markova *et al.* 2008). Thus, the transmembrane ratio for Cl is approximately 10-fold, by contrast, for instance, to Ca ions, where this ratio is approximately 10 000-fold.

The second difficulty is associated with the fact that the E_{Cl} is close to the resting potential of the cells. Depending on the cell type and the stage of development, the E_{Cl} may be either positive (in this case increase of Cl permeability leads to depolarization) or negative relative to the resting potential (in which case an increase of the Cl permeability leads to hyperpolarization). As a result, in normal physiological conditions, the driving force at the resting potential rarely exceeds 20 mV. Thus, for reliable $[Cl]_i$ monitoring, one has to use highly sensitive probes.

Among several methods proposed for intracellular Cl recording, the use of quinoline-based Cl-sensitive fluorescent dyes is presently the most widespread. This method has been used for monitoring the changes of Cl in a variety of preparations, including isolated growth cones, neurons, glia, different types of epithelial cells, fibroblasts and pancreatic β-cells (see references in Mansoura *et al.* (1999), Chub *et al.* (2006) and Painter & Wang (2006)). These compounds have low biological toxicity, a rapid response to changes in Cl and a relatively good sensitivity to Cl. However, they are prone to a time-dependent decay in fluorescence owing to the gradual leakage of dye from the labelled cells or bleaching (Krapf *et al.* 1988; Biwersi & Verkman 1991; Inglefield & Schwartz-Bloom 1997; Nakamura *et al.* 1997; Chub *et al.* 2006; Painter & Wang 2006).

Genetically encoded fluorescent probes are powerful tools for visualization of Cl ions in live cells (Kuner & Augustine 2000; Galietta *et al.* 2001*b*; Metzger *et al.* 2002; Slemmer *et al.* 2004; Duebel *et al.* 2006; Markova *et al.* 2008). In contrast to quinoline-based Cl-sensitive dyes, YFP-based probes allow long-lasting (hours) highly reproducible monitoring of Cl. However, these proteins are less Cl sensitive than quinoline-based dyes (Biwersi & Verkman 1991; Schwartz & Yu 1995). In addition, YFP-based proteins are pH sensitive (Kuner & Augustine 2000; Markova *et al.* 2008) and they exhibit relatively slow (approx. 100 ms) binding kinetics to Cl (Jayaraman *et al.* 2000).

In this study, we describe experiments on using the recently developed Cl-Sensor with high Cl sensitivity (Markova *et al.* 2008) and a new genetically encoded indicator for monitoring the activation of Cl-selective GlyR channels. In comparison with the previously described molecules, our Cl-Sensor, due to mutations in the YFP, exhibits approximately fivefold higher sensitivity to Cl. For instance, the K_{app} for Clomeleon (Kuner & Augustine 2000) is greater than 160 mM, while for Cl-Sensor $K_{app} = 30$ mM (Markova *et al.* 2008). The second advantage of Cl-Sensor is the possibility of ratiometric monitoring at alternating excitation wavelengths; that is, it can be used as an excitation ratiometric indicator on set-ups equipped with devices for a rapid change of excitation wavelength.

For Cl-Sensor gene delivering to retinal cells, we used *in vivo* electroporation techniques (Matsuda & Cepko 2004). Our experiments demonstrated that the efficiency of electroporation in the developing post-natal retina (at P0) is high, and that the transgenic expression persists for more than one month. Moreover, compared with other gene transfer methods, such as viral vectors, *in vivo* electroporation has several advantages. First, it allows the introduction in retina cells of various types of cDNA constructs prepared for conventional cell transfection. Second, several different DNA constructs can be introduced into the same cells at once (Matsuda & Cepko 2004, 2007). We demonstrated that

in vivo electroporation of Cl-Sensor cDNA is a powerful tool for monitoring $[Cl]_i$ at different experimental conditions and at age-dependent changes of Cl in neurons.

The second construct, BioSensor-GlyR, is a GlyR channel protein with Cl-Sensor incorporated into the long cytoplasmic domain. Insertion was performed in the region of GlyR, thus preserving the functional properties of the receptor. As a result, we obtained a new probe for spectroscopic monitoring of GlyR channel activation in live cells.

Our preliminary analysis suggests that the sensitivity of BioSensor-GlyR is high enough to resolve changes in $[Cl]_i$ induced by the activation of postsynaptic receptors in glycinergic synapses. The decay kinetics of the fluorescence responses is slow in comparison with ionic currents. This is partially due to the kinetics of Cl binding by YFP. While the I152L mutation strongly accelerates the binding and dissociation kinetics (Galietta *et al.* 2001*a*), the chromophore response is still relatively slow.

Another factor retarding the kinetics is the distribution of BioSensor-GlyR in cells. Only some of the protein molecules are incorporated in the surface membrane of the recorded cells, while those molecules of BioSensor-GlyR situated in the cytoplasmic compartments respond with a delay following the changes in Cl concentration in the cell's volume. In transgenic animals, expression of BioSensor-GlyR in specific areas of glycinergic synapses should diminish this problem.

In spite of these limitations, BioSensor-GlyR, the first genetically encoded indicator for non-invasive monitoring of receptor-operated channels, represents a promising tool for analysis of activity dependences and pharmacological challenges in cells expressing these receptors.

Development of transgenic animals expressing Cl-Sensor and BioSensor-GlyR will be useful for studies of Cl-driven inhibitory neuronal networks, Cl homeostasis and dysfunction of Cl-selective channels in cell culture systems, brain slice preparations and intact tissues. Transgenic mouse lines carrying the gene for YFP and for the CFP–YFP construct have already been successfully used for estimation of the Cl distribution in bipolar cells of the retina (Duebel *et al.* 2006) and analysis of the effects of glutamate on intracellular Cl elevation in hippocampal neurons (Metzger *et al.* 2002; Slemmer *et al.* 2004). As Cl-Sensor constructs exhibit several times higher sensitivity to Cl than does YFP, transgenic animals expressing Cl-Sensor and BioSensor-GlyR promise to provide more sensitive models.

In many cases, changes in Cl take place in local environments. For instance, at the activation of Cl-selective channels, the main changes in Cl concentration take place close to the cellular plasma membrane. Previously proposed Cl indicators do not allow direct monitoring of these near-membrane Cl fluxes, as fluorescent dyes are homogeneously distributed in the cytoplasm and thus allow detection of only the mean change in Cl concentration over the whole volume of the cell.

By contrast, BioSensor-GlyR provides the possibility for genetically targeted expression with transmembrane protein and thus allows monitoring of Cl changes in the local surroundings of GlyR channels. A similar strategy can be used for other anion-selective channels. Particularly promising is the development of indicators for non-invasive monitoring of $GABA_A$ receptors with Cl-Sensor incorporated in the cytoplasmic loop of its subunits. This would allow,

for instance, the estimation of Cl in local synaptic areas of different neurons and its changes during different patterns of neuronal network activity.

In adult nervous systems of vertebrates, the main inhibitory drive is performed via activation of Cl-selective $GABA_A$ receptor channels. Owing to low $[Cl]_i$, opening of these receptors generates a membrane hyperpolarization and a reduction in action potential firing. By contrast, in immature neurons $[Cl]_i$ is elevated and consequently release of GABA leads to membrane depolarization, i.e. this neurotransmitter is primarily excitatory (Ben-Ari *et al.* 2007). The key role in the regulation of $[Cl]_i$ during neuronal development is played by specific Cl transporters, NKCC1 and NKCC2 (isoforms of the Na–K–Cl cotransporter; Payne *et al.* 2003). However, detailed mechanisms of these changes in Cl homeostasis need clarification. Using transgenic animals expressing Cl-Sensor fused with $GABA_A$ receptors could be an effective approach for this analysis.

Using specific promoters for expressing BioSensors for GlyR and γ-aminobutyric acid receptor in certain cellular subpopulations promises to be useful for screening pharmacological agents in the treatment of disorders resulting from the disturbance of Cl homeostasis and dysfunctions involving inhibitory neurotransmission.

We wish to thank Dr I. Medina for his help with some experiments. We thank also C. Pellegrino for his help with some cultures and Dr G. Haase for BTX electroporator. This work was supported by the French Association against Myopathies (AFM) for M.M., by a fellowship from the French Ministry of Foreign Affairs for O.M. and by the NEUROCYPRES grant from the European Commission Seventh Framework Programme for S.B. and P.B.

References

Ashcroft, F. M. 2000 *Ion channels and diseases*. San Diego, CA: Academic Press.

Becker, C. M. 1990 Disorders of the inhibitory glycine receptor: the spastic mouse. *FASEB J.* **4**, 2767–2774.

Ben-Ari, Y., Gaiarsa, J. L., Tyzio, R. & Khazipov, R. 2007 GABA: a pioneer transmitter that excites immature neurons and generates primitive oscillations. *Physiol. Rev.* **87**, 1215–1284. (doi:10.1152/physrev.00017.2006)

Biwersi, J. & Verkman, A. S. 1991 Cell-permeable fluorescent indicator for cytosolic chloride. *Biochemistry* **30**, 7879–7883. (doi:10.1021/bi00246a001)

Borodinsky, L. N. & Spitzer, N. C. 2007 Activity-dependent neurotransmitter–receptor matching at the neuromuscular junction. *Proc. Natl Acad. Sci. USA* **104**, 335–340. (doi:10.1073/pnas.0607450104)

Chub, N., Mentis, G. Z. & O'donovan, M. J. 2006 Chloride-sensitive MEQ fluorescence in chick embryo motoneurons following manipulations of chloride and during spontaneous network activity. *J. Neurophysiol.* **95**, 323–330. (doi:10.1152/jn.00162.2005)

Chudotvorova, I., Ivanov, A., Rama, S., Hübner, C. A., Pellegrino, C., Ben-Ari, Y. & Medina, I. 2005 Early expression of KCC2 in rat hippocampal cultures augments expression of functional GABA synapses. *J. Physiol.* **566**, 671–679. (doi:10.1113/jphysiol.2005.089821)

David-Watine, B., Shorte, S. L., Fucile, S., De Saint Jan, D., Korn, H. & Bregestovski, P. 1999 Functional integrity of green fluorescent protein conjugated glycine receptor channels. *Neuropharmacology* **38**, 785–792. (doi:10.1016/S0028-3908(99)00015-5)

Demaurex, N. & Frieden, M. 2003 Measurements of the free luminal ER Ca^{2+} concentration with targeted "cameleon" fluorescent proteins. *Cell Calcium* **34**, 109–119. (doi:10.1016/S0143-4160(03)00081-2)

Duebel, J., Haverkamp, S., Schleich, W., Feng, G., Augustine, G. J., Kuner, T. & Euler, T. 2006 Two-photon imaging reveals somatodendritic chloride gradient in retinal ON-type bipolar cells expressing the biosensor clomeleon. *Neuron* **49**, 81–94. (doi:10.1016/j.neuron.2005.10.035)

Fucile, S., De Saint Jan, D., de Carvalho, L. P. & Bregestovski, P. 2000 Fast potentiation of glycine receptor channels by intracellular calcium in neurons and transfected cells. *Neuron* **28**, 571–583. (doi:10.1016/S0896-6273(00)00134-3)

Galietta, L. V. J., Haggie, P. M. & Verkman, A. S. 2001*a* Green fluorescent protein-based halide indicators with improved chloride and iodide affinities. *FEBS Lett.* **499**, 220–224. (doi:10.1016/S0014-5793(01)02561-3)

Galietta, L. V. J., Jayaraman, S. & Verkman, A. S. 2001*b* Cell-based assay for high-throughput quantitative screening of CFTR chloride transport agonists. *Am. J. Physiol. Cell Physiol.* **281**, C1734–C1742.

Gandhi, C. S., Loots, E. & Isacoff, E. Y. 2000 Reconstructing voltage sensor–pore interaction from a fluorescence scan of a voltage-gated K^+ channel. *Neuron* **27**, 585–595. (doi:10.1016/S0896-6273(00)00068-4)

Ghavanini, A. A., Mathers, D. A., Kim, H. S. & Puil, E. 2006 Distinctive glycinergic currents with fast and slow kinetics in thalamus. *J. Neurophysiol.* **95**, 3438–3448. (doi:10.1152/jn.01218.2005)

Gorostiza, P., Volgraf, M., Numano, R., Szobota, S., Trauner, D. & Isacoff, E. Y. 2007 Mechanisms of photoswitch conjugation and light activation of an ionotropic glutamate receptor. *Proc. Natl Acad. Sci. USA* **104**, 10 865–10 870. (doi:10.1073/pnas.0701274104)

Hamill, O. P., Bormann, J. & Sakmann, B. 1983 Activation of multiple-conductance state chloride channels in spinal neurones by glycine and GABA. *Nature* **305**, 805–808. (doi:10.1038/305805a0)

Inglefield, J. R. & Schwartz-Bloom, R. D. 1997 Confocal imaging of intracellular chloride in living brain slices: measurement of $GABA_A$ receptor activity. *J. Neurosci. Methods* **75**, 127–135. (doi:10.1016/S0165-0270(97)00054-X)

Jayaraman, S., Haggie, P., Wachter, R. M., Remington, S. J. & Verkman, A. S. 2000 Mechanism and cellular applications of a green fluorescent protein-based halide sensor. *J. Biol. Chem.* **275**, 6047–6050. (doi:10.1074/jbc.275.9.6047)

Kere, J., Lohi, H. & Hoglund, P. 1999 Genetic disorders of membrane transport III. Congenital chloride diarrhea. *Am. J. Physiol.* **276**, G7–G13.

Koch, M. C. *et al.* 1992 The skeletal muscle chloride channel in dominant and recessive human myotonia. *Science* **257**, 797–800. (doi:10.1126/science.1379744)

Krapf, R., Berry, C. A. & Verkman, A. S. 1988 Estimation of intracellular chloride activity in isolated perfused rabbit proximal convoluted tubules using a fluorescent indicator. *Biophys. J.* **53**, 955–962.

Kruger, W., Gilbert, D., Hawthorne, R., Hryciw, D. H., Frings, S., Poronnik, P. & Lynch, J. W. 2005 A yellow fluorescent protein-based assay for high-throughput screening of glycine and $GABA_A$ receptor chloride channels. *Neurosci. Lett.* **380**, 340–345. (doi:10.1016/j.neulet.2005.01.065)

Kuner, T. & Augustine, G. J. 2000 A genetically encoded ratiometric indicator for chloride: capturing chloride transients in cultured hippocampal neurons. *Neuron* **27**, 447–459. (doi:10.1016/S0896-6273(00)00056-8)

Lloyd, S. E. *et al.* 1996 A common molecular basis for three inherited kidney stone diseases. *Nature* **379**, 445–449. (doi:10.1038/379445a0)

Mansoura, M. K., Biwersi, J., Ashlock, M. A. & Verkman, A. S. 1999 Fluorescent chloride indicators to assess the efficacy of CFTR cDNA delivery. *Hum. Gene Ther.* **10**, 861–875. (doi:10.1089/10430349950018274)

Markova, O., Mukhtarov, M., Real, E., Jacob, Y. & Bregestovski, P. 2008 Genetically encoded chloride indicator with improved sensitivity. *J. Neurosci. Methods* **170**, 67–76. (doi:10.1016/j.jneumeth.2007.12.016)

Matsuda, T. & Cepko, C. L. 2004 Electroporation and RNA interference in the rodent retina *in vivo* and *in vitro*. *Proc. Natl Acad. Sci. USA* **101**, 16–22. (doi:10.1073/pnas.2235688100)

Matsuda, T. & Cepko, C. L. 2007 Controlled expression of transgenes introduced by *in vivo* electroporation. *Proc. Natl Acad. Sci. USA* **104**, 1027–1032. (doi:10.1073/pnas.0610155104)

Metzger, F. *et al.* 2002 Transgenic mice expressing a pH and Cl^- sensing yellow-fluorescent protein under the control of a potassium channel promoter. *Eur. J. Neurosci.* **15**, 40–50. (doi:10.1046/j.0953-816x.2001.01837.x)

Miyawaki, A. 2003 Fluorescence imaging of physiological activity in complex systems using GFP-based probes. *Curr. Opin. Neurobiol.* **13**, 591–596. (doi:10.1016/j.conb.2003.09.005)

Mukhtarov, M., Ragozzino, D. & Bregestovski, P. 2005 Dual Ca^{2+} modulation of glycinergic synaptic currents in rodent hypoglossal motoneurons. *J. Physiol.* **569**, 817–831. (doi:10.1113/jphysiol.2005.094862)

Nakamura, T., Kaneko, H. & Nishida, N. 1997 Direct measurement of the chloride concentration in newt olfactory receptors with the fluorescent probe. *Neurosci. Lett.* **237**, 5–8. (doi:10.1016/S0304-3940(97)00794-5)

Ortells, M. O. & Lunt, G. G. 1995 Evolutionary history of the ligand-gated ion-channel superfamily of receptors. *Trends Neurosci.* **18**, 121–127. (doi:10.1016/0166-2236(95)93887-4)

Painter, R. G. & Wang, G. 2006 Direct measurement of free chloride concentrations in the phagolysosomes of human neutrophils. *Anal. Chem.* **78**, 3133–3137. (doi:10.1021/ac0521706)

Payne, J. A., Rivera, C., Voipio, J. & Kaila, K. 2003 Cation-chloride cotransporters in neuronal communication, development and trauma. *Trends Neurosci.* **26**, 199–206. (doi:10.1016/S0166-2236(03)00068-7)

Rhoden, K. J., Cianchetta, S., Stivani, V., Portulano, C., Galietta, L. J. V. & Romeo, G. 2007 Cell-based imaging of sodium iodide symporter activity with the yellow fluorescent protein variant YFP-H148Q/I152L. *Am. J. Physiol. Cell Physiol.* **292**, C814–C823. (doi:10.1152/ajpcell.00291.2006)

Rohrbough, J. & Spitzer, N. C. 1996 Regulation of intracellular Cl^- levels by Na^+-dependent Cl^- cotransport distinguishes depolarizing from hyperpolarizing $GABA_A$ receptor-mediated responses in spinal neurons. *J. Neurosci.* **16**, 82–91.

Schwartz, R. D. & Yu, X. 1995 Optical imaging of intracellular chloride in living brain slices. *J. Neurosci. Methods* **62**, 185–192. (doi:10.1016/0165-0270(95)00075-5)

Shiang, R., Ryan, S. G., Zhu, Y. Z., Hahn, A. F., O'Connell, P. & Wasmuth, J. J. 1993 Mutations in the α 1 subunit of the inhibitory glycine receptor cause the dominant neurologic disorder, hyperekplexia. *Nat. Genet.* **5**, 351–358. (doi:10.1038/ng1293-351)

Siegel, M. S. & Isacoff, E. Y. 1997 A genetically encoded optical probe of membrane voltage. *Neuron* **19**, 735–741. (doi:10.1016/S0896-6273(00)80955-1)

Simon, D. B. & Lifton, R. P. 1996 The molecular basis of inherited hypokalemic alkalosis: Bartter's and Gitelman's syndromes. *Am. J. Physiol.* **271**, F961–F966.

Slemmer, J. E., Matsushita, S., De Zeeuw, C. I., Weber, J. T. & Knöpfel, T. 2004 Glutamate-induced elevations in intracellular chloride concentration in hippocampal cell cultures derived from EYFP-expressing mice. *Eur. J. Neurosci.* **19**, 2915–2922. (doi:10.1111/j.0953-816X.2004.03422.x)

Thoreson, W. B. & Bryson, E. J. 2004 Chloride equilibrium potential in salamander cones. *BMC Neurosci.* **5**, 53. (doi:10.1186/1471-2202-5-53)

Thoreson, W. B., Stella Jr, S. L., Bryson, E. I., Clements, J. & Witkovsky, P. 2002 D_2-like dopamine receptors promote interactions between calcium and chloride channels that diminish rod synaptic transfer in the salamander retina. *Vis. Neurosci.* **19**, 235–247. (doi:10.1017/S0952523802192017)

Treiman, D. M. 2001 GABAergic mechanisms in epilepsy. *Epilepsia* **42**, 8–12. (doi:10.1046/j.1528-1157.2001.042suppl.3008.x)

Tyzio, R., Cossart, R., Khalilov, I., Minlebaev, M., Hubner, C. A., Represa, A., Ben-Ari, Y. & Khazipov, R. 2006 Maternal oxytocin triggers a transient inhibitory switch in GABA signaling in the fetal brain during delivery. *Science* **314**, 1788–1792. (doi:10.1126/science.1133212)

Tyzio, R., Holmes, G. L., Ben-Ari, Y. & Khazipov, R. 2007 Timing of the developmental switch in $GABA_A$ mediated signaling from excitation to inhibition in CA3 rat hippocampus using gramicidin perforated patch and extracellular recordings. *Epilepsia* **48**, 96–105. (doi:10.1111/j.1528-1167.2007.01295.x)

Wachter, R. M. & Remington, S. J. 1999 Sensitivity of the yellow variant of green fluorescent protein to halides and nitrate. *Curr. Biol.* **9**, R628–R629. (doi:10.1016/S0960-9822(99)80408-4)